Forschung im Ingenieurwesen (2024)88:1
https://doi.org/10.1007/s10010-023-00721-3

ORIGINALARBEITEN/ORIGINALS

Spur gear teeth reconstruction via direct laser deposition

P. C. Romio[1,2] · P. M. T. Marques[2] · J. H. O. Seabra[1,2] · C. M. C. G. Fernandes[1,2] · J. Gil[2] · R. Cardoso[2] · M. F. Vieira[1,2] · J. M. Cruz[3]

Received: 13 March 2023 / Accepted: 19 November 2023

Abstract

Fatigue damage, such as pitting and tooth root fatigue fracture, is one of several gear failure modes encountered in practical applications. Some of these failure modes are traditionally repairable, while others are known to be catastrophic and unrepairable. Direct Laser Deposition (DLD) is a Metal Additive Manufacturing process that could overcome this problem and extend the useful gear life. The DLD repair process proved to be applicable in several cases. Nevertheless, concrete applications for gears are still scarce and limited to preset teeth reconstruction without discussing functional applications. Based on that perspective, this research aims to evaluate the DLD performance of a gear under actual operation. This work details the strategy applied to restore a base material case-hardened 16 MnCr 5 FZG-C Type C-GF pinion using a DLD combination of pure Inconel 625 (MetcoClad 625) for the tooth core and pure AISI 431 (Metco 42C) as a superficial coating. The pinion was tested for over 2.7 million cycles under different load stages (K1 to K9), functionally resisting until a static torque of 215.6 Nm, although it presented severe surface damage development throughout the campaign. This exploratory work thoroughly discusses the drawbacks encountered in the repair process, materials characterization, surface evolution of the restored teeth against base material, and mass loss during the tests.

Rekonstruktion der Stirnradverzahnung mittels direkter Laserauftragung

Zusammenfassung

Ermüdungsschäden, wie z. B. Graufleckigkeit und Zahnfußermüdungsbruch, sind eine von mehreren Getriebeausfallarten, die in praktischen Anwendungen auftreten. Einige dieser Ausfallarten sind traditionell reparierbar, während andere als katastrophal und nicht reparierbar bekannt sind. Die Reparatur durch direkte Laserabscheidung (DLD) ist ein additives Fertigungsverfahren, das diese Probleme überwinden und die Lebensdauer des Getriebes verlängern könnte. Das DLD-Reparaturverfahren hat sich in mehreren Fällen als anwendbar erwiesen, von Schienen bis zu Zahnrädern. Dennoch sind konkrete Anwendungen für Zahnräder noch rar und beschränken sich auf die Rekonstruktion von Zähnen, ohne funktionelle Anwendungen zu diskutieren. Basierend auf dieser Perspektive zielt diese Forschungsarbeit darauf ab, die DLD-Reparaturleistung eines FZG-Getriebes unter realem Betrieb zu bewerten. Diese Arbeit beschreibt die Strategie zur Wiederherstellung eines einsatzgehärteten 16 MnCr 5 FZG-Typ-C-Ritzels aus Grundmaterial unter Verwendung einer DLD-Kombination aus reinem Inconel 625 (MetcoClad 625) für den Zahnkern und reinem AISI 431 (Metco 42C) als Oberflächenbeschichtung. Das Ritzel wurde über 2,7 Mio Zyklen in verschiedenen Belastungsstufen (K1 bis K9) getestet und hielt bis zu einem Drehmoment von 215,6 Nm funktionell stand, obwohl es während der gesamten Versuche Oberflächenschäden aufwies. Diese explorative Arbeit diskutiert gründlich die Nachteile, die beim Reparaturprozess, der Materialcharakterisierung, der Oberflächenentwicklung der reparierten Zähne gegenüber dem Basismaterial und dem Masseverlust während der Tests aufgetreten sind.

✉ P. C. Romio
pedro.romio@gmail.com

[1] FEUP, Porto, Portugal

[2] INEGI, Porto, Portugal

[3] SERMEC Group, Porto, Portugal

1 Introduction

International Standard ISO 10825-1 [1] categorizes the most common failure modes in gears into six classes: (1) Tribological damage (non-fatigue) (e.g., abrasive wear and scuffing); (2) Fatigue damage (e.g., pitting and tooth root fatigue fracture); (3) Non-fatigue fracture (e.g., tooth root rupture and tooth shear fracture); (4) Plastic deformation (e.g., indentation and fracture after plastic deformation); (5) Manufacturing issues (e.g., hardening cracks and case/core separation); (6) Other surface damage (e.g., corrosion and cavitation).

Some of these failure modes, like micropitting, might be repaired using conventional methods, such as regrinding or surface finishing. The processes eliminate surface failures by removing material from the tooth surface [2, 3]. The problem is that material removal has a limit and affects tooth geometry. At some point, it becomes impossible to repair the gear while keeping the required geometric tolerances and performance, leading to its substitution (sometimes too soon). Other failure modes in this list, such as tooth root fatigue fracture, are known to be catastrophic and immediately take the system out of operation.

In recent years, an approach driven by advances in Metal Additive Manufacturing (MAM) started being considered to overcome the problem and extend the useful gear life. This repair process can be generically described in three steps: (1) the cleaning step, where using polishing, abrasive blasting, or machining, the damaged surface or volume is cleaned (similar to the traditional methods); (2) the filling step, where the cleaned-up area is filled with a deposition material; and (3) the finishing step, which restores the deposition zone to its original shape and size [4].

MAM repairs hold two distinct classes: (1) geometric restoration and (2) structural repair. For the first, the deposited material aims to restore the component geometry, function and surface finish properties but is not expected to carry structural loads. In the second, the deposited material must restore the part's geometry and strength capabilities under static or dynamic loading. Among the available MAM processes employed in metallic components repair, one that has proven particularly useful is the Direct Laser Deposition (DLD) process. The DLD has been applied to both classes on repairing high-value parts that used to be not repairable or that presented some impediment, such as too small parts that could be affected by the Heat Affected Zone (HAZ) [5].

DLD combines the material and energy delivery in the layer-by-layer formation, as illustrated in Fig. 1. The deposition material is available in two forms: wire and powder, with powder favoured and supported by the most recent DLD machines. The current generation of DLD machines may contain up to four (or more) nozzles, allowing diverse alloy combinations, with inert gas protection, reducing the oxidation resulting from the high metal processing temperature [8]. The success of DLD in some repair operations is directly related to: (1) Narrow HAZ during the process; (2) High resolution that allows repair with high precision; (3) High metallurgical integrity of the produced parts; (4) Capacity to provide better material properties; (5) Suitability for full automation; (6) Higher repeatability [6, 7].

The DLD applications are numerous, including the repair of turbine blades, sintered tools, steam circuit parts of a thermal power station, marine crankshaft, dies, rails, gas turbine burners, compressor seals, engine turbine shaft, four-stroke pistons, spur gears [4, 6, 7]. Nevertheless, the application of DLD regarding gear repair is still scarce in the literature and focuses mainly on the tooth reconstruction aspects and mechanical characterization, such as hardness and tensile strength [9–12]. However, very little is presented concerning actual operational results.

As an example, Shi and Bai [9] reconstructed a C45 steel gear thermal refined using a Ni45 alloy powder and evaluated three different deposition schemes, illustrated in Fig. 2. In Scheme 1, the deposition started in the gear tooth root, and two other tracks overlapped along the top tooth direction. For Scheme 2, the first track was deposited in the gear tooth root, the second track in the top of the gear tooth and the third track between the other two. Finally, in Scheme 3, the first track was applied in the gear tooth top, the second in the root and the last in between [9]. The authors analyzed the microstructure and hardness of the reconstructed teeth, concluding that the deposited layers' properties were superior to the substrate, the restored teeth presented small HAZ, and DLD could be used to repair complex surfaces like those existing in gear teeth. On the other hand, the authors did not obtain an involute profile using DLD and did not test the gears.

Zhu et al. [10] also presented a reconstruction strategy for a C45 steel gear using AISI H13 steel powder, as shown in Fig. 3. However, in order to perform mechanical tests, a set of samples was produced using the same parameters applied to the tooth. The authors evaluate microstructure, hardness, tensile behaviour and wear resistance. They concluded that the reconstructed tooth presents a lower tensile strength but a higher hardness and better wear resistance than the original tooth. After post-processing, the authors did not perform functional tests.

Bons [11] is another author who evaluated the gear tooth reconstruction from a sample perspective, as indicated in Fig. 4. In his work, 18 CrNiMo 7-6 steel was used as the base material, Inconel 718 was deposited as a tooth core, and NT-NI60 was applied as a coating. In addition, the author performed hardness and static load tests to compare the reconstructed tooth against the base material-only tooth.

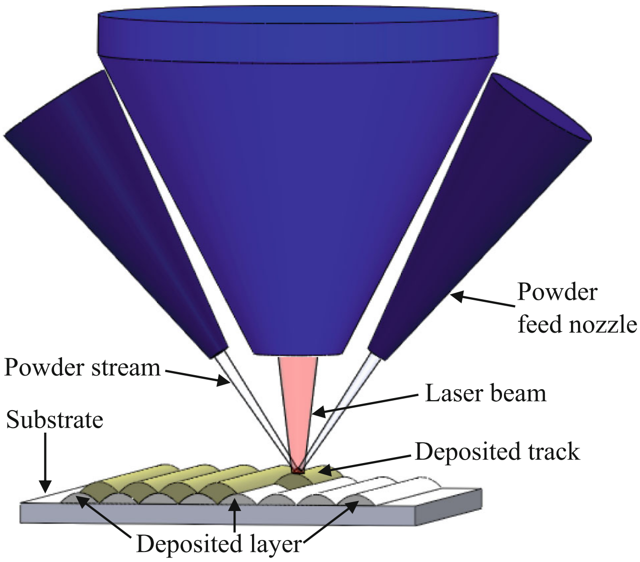

Fig. 1 DLD process using a laser beam as an energy source

The results show that the DLD teeth showed worse mechanical properties than the reference 18 CrNiMo 7-6 steel.

Finally, Guan et al. [12] investigated the reconstruction process of a broken 20 CrMnTi gear using Ni60 as-deposited material. The study evaluates different deposition strategies in order to rebuild a gear tooth and repair a gear using the optimized parameters found, as illustrated in Fig. 5. The phase composition, microstructure, hardness, and wear properties of the restored gear tooth were analyzed by X-ray diffraction (XRD), Scanning Electron Microscopy (SEM), microhardness tester, and friction and wear tester. Using a test sample cut from the gear, the authors concluded that the teeth presented a good metallurgical bond with the substrate and hardness compatible with base material values. Once more, the gear was not put into operation.

From the current survey, it is safe to say that functional DLD-repaired gears are not presented in technical literature, and there is a lack of information regarding operational behaviour. In fact, up to now, there is no work showing a gear reconstructed via DLD under operation. The drawbacks related to tooth geometry and mechanical resistance still hinder actual applications. In this sense, this exploratory work presents in detail the strategy used to restore a base material case-hardened 16 MnCr 5 FZG-C Type C-GF pinion using a DLD combination of pure Inconel 625 (MetcoClad 625) for the tooth core and pure AISI 431 (Metco 42C) as a superficial coating, but also tested the reconstructed pinion for more than 2.7 million cycles under different load stages, up to 215.6 Nm. The surface topography evaluation (visual registration and tooth flank roughness assessment) of the restored and the base material teeth throughout the tests allows a performance comparison of the teeth under the same operational condition.

This work is part of a broader research project called GEAR 3D (POCI-01-0247-FEDER-039848) [13], which aims to develop a methodology for 3D reconstruction of large-dimension case-hardened gear teeth for the wind sector. Among the project purposes, one must emphasize: (1) study deposition strategies, (2) exploit synergies of different material properties to obtain a repaired gear tooth with the required characteristics, and (3) development of test protocols to validate the quality/reliability of gear repair using DLD technology, in particular fatigue damage (pitting and tooth root fatigue fracture). The first two parts of this project identified the two potential materials (Inconel 625 and AISI 431) through evaluation of their properties in deposited form and specimen testing in lab conditions (microhardness, tensile tests, abrasive wear, SEM, rolling contact fatigue) and their required DLD process parameters to reconstruct gear teeth [14–19]. The results show that Inconel 625 easily develops heights during the deposition, unlike AISI 413. On the other hand, the reduced hardness of Inconel 625 motivated the choice of a coating that would allow better wear resistance. From this first study by the research group, the presented strategy in this paper was developed and applied to teeth restoration. In this context, the current analysis intends to evaluate how this particular combination of materials would perform under real applications, investigating two major aspects: tooth root resistance and flank durability. Certainly, there are other important aspects concerning gear tooth reconstruction (for example, automation of the DLD process or economic efficiency) that should also be evaluated and discussed in order to assess DLD repair capabilities. However, they are out of

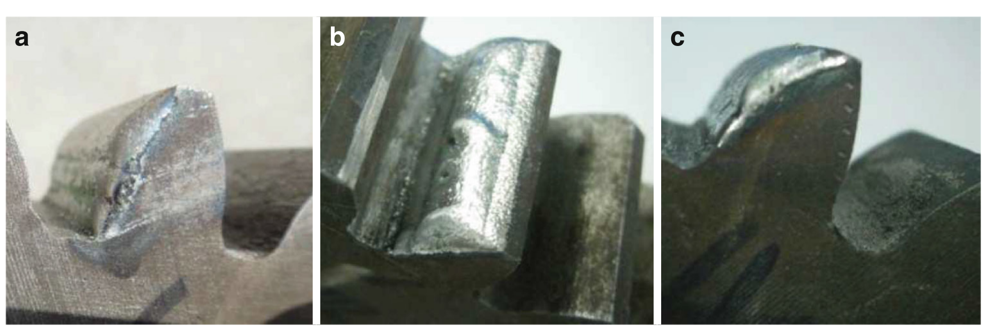

Fig. 2 The results of three schemes of laser cladding test on the tooth surface. **a** Scheme 1, **b** Scheme 2 and **c** Scheme 3. Adapted from [9]

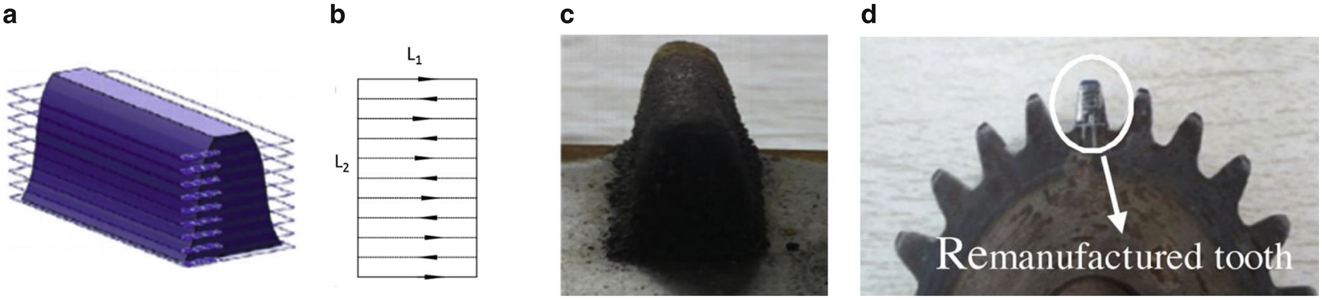

Fig. 3 Broken gear tooth repairing process: **a** slices of the broken tooth model, **b** the shape of the first layer of the broken tooth model slices, **c** remanufactured tooth using DLD, **d** remanufactured tooth after post-processing. Adapted from [10]

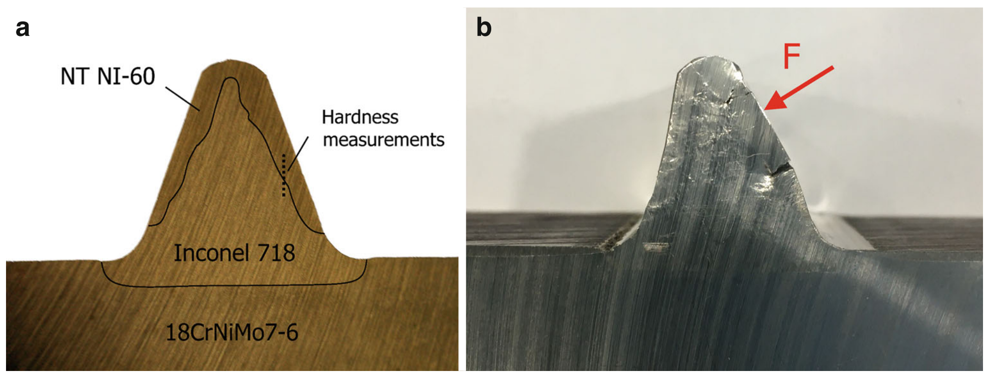

Fig. 4 Test sample for gear tooth reconstruction evaluation: **a** materials applied to the repair and **b** sample after a static load test. Adapted from [11]

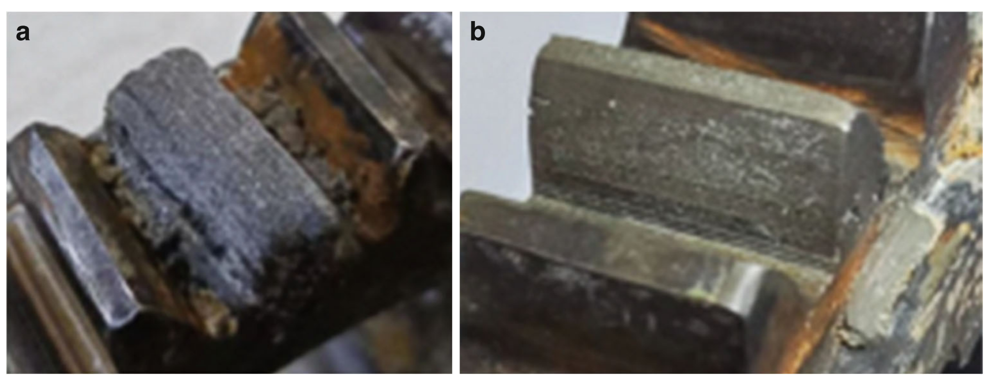

Fig. 5 20 CrMnTi gear repair using Ni60: (**a**) Direct Laser Deposition of Ni60 and (**b**) tooth shape restoration using a mill process. Adapted from [12]

this work scope and will not be analysed in this paper. In this exploratory work, only the functional behaviour is investigated.

2 Materials and methods

2.1 DLD reconstructed gear

In order to evaluate the DLD performance under operational conditions, an FZG-C Type C-GF pinion, detailed in Table 1 [20], had three teeth removed and then reconstructed by DLD, as illustrated in Fig. 6.

Teeth 1 and 9 were entirely removed from the pinion, while tooth 3 was partially cut over the pitch line to the tip tooth (Fig. 6a) using a conventional face milling process. Teeth 5, 11 and 13 were chosen for base material control and to establish the reference for the comparison between the as-built by conventional processes and DLD. The adopted strategy for the teeth reconstruction consisted of a combination of pure Inconel 625 (MetcoClad 625) for the tooth core and pure AISI 431 (Metco 42C) as a superficial coating. Table 2 presents the nominal weight percentage for the chemical composition of such materials.

For teeth 1 and 9, seven layers were used. The DLD routine is illustrated in Fig. 7. As one can see, for five layers, an external perimeter of AISI 413 was initially deposited, followed by filling the tooth core with Inconel 625. The last two layers used only AISI 413 for both perimeter and filling. The theoretical dimensions of the prism were 8.5 (width) × 14.5 (length) × 12 mm (height). The laser scanning pattern rotated 90 ∘ between layers, as shown in Fig. 7c and d, and the starting point of each layer was randomly chosen in order to better distribute the thermal delivery over the part—starting the deposit in the same position may lead to "slump" problems.

Figure 6b presents the obtained result with the DLD process. Tooth 3 followed a similar DLD approach but only used three layers. The first layer combines Inconel 625 and AISI 413, while the last two were made only with AISI 413. The theoretical dimensions of the prism were 9 (width) × 14 (length) × 5.4 mm (height).

An essential aspect of DLD concerns the parameters used in the deposition. Table 3 summarizes what was used in this work. The presented values were the same for both materials, except for the carrier gas rate, since the AISI 413 is less spherical and requires more transport flow. These particular value choices rely on the results from previous studies [14–16]. The laser system (LDF 3000–100) has a high-power fibre-coupled laser diode (wavelength 900–1030 nm, depending on the power) with a nominal beam power of 6000 W. The machine concept is a KUKA KR90 R3100 industrial robot based on a 6-axis industrial robot. All axes are connected to the robot and laser control units, which command the temperature of the melt pool as well as the laser power. A coaxial feeding system fed the powder during deposition.

Finally, the tooth's involute profile (Fig. 6c) was achieved by employing wire Electrical Discharge Machining (EDM), with the trajectory defined by digitizing one of the base material teeth. In this case, the tolerances were determined by the post-processing operation. The base tangent length over three gear teeth (W_k) was used as a reference in the current evaluation. At all teeth positions, the measurements were inside the allowed tolerance (Table 1). Since only one reconstructed gear sample was available, a statistical study on the variability of the post-processing reconstruction was not performed.

It is also worth highlighting that similar gears, produced by the same process, presented a gear quality grade of 12, according to DIN 3962. This analysis is illustrated in Fig. 8, where one can observe the Range of tooth thickness errors (R_s) equal to 0.164 mm in an FZG-C Type C-GF pinion with four reconstructed teeth (1, 5, 9 and 13). This result is particularly significant since it illustrates how rebuilt teeth

Table 1 Gear geometry FZG-C, type C-GF [20]

Dimension		Numerical value
Centre distance		91.5 mm
Effective tooth width		14.0 mm
Working pitch diameter	*Pinion*	73.2 mm
	Wheel	109.8 mm
Tip diameter	*Pinion*	$82.46^{-0.087}$ mm
	Wheel	$118.36^{-0.087}$ mm
Module		4.5 mm
Number of teeth	*Pinion*	16
	Wheel	24
Addendum modification factor	*Pinion*	0.1817
	Wheel	0.1715
Pressure angle		20.0°
Working pressure angle		22.4°
Helix angle		0.0°
Tooth correction		Without tip relief and root relief, no longitudinal crowning
Material		16 MnCr 5 according to DIN 17210
Heat treatment		The test gears are case-carburized, surface hardness 750 HV1, in the area of the tooth flank
Gear quality grade		5 according to DIN 3962
	Span of pinion	$34.779^{-0.011}_{-0.135}$ mm, measured over three teeth
	Span of wheel	$35.252^{-0.011}_{-0.135}$ mm, measured over three teeth
Average roughness of tooth flanks		0.5 ± 0.1 µm
Grinding		Maag 0°—grinding

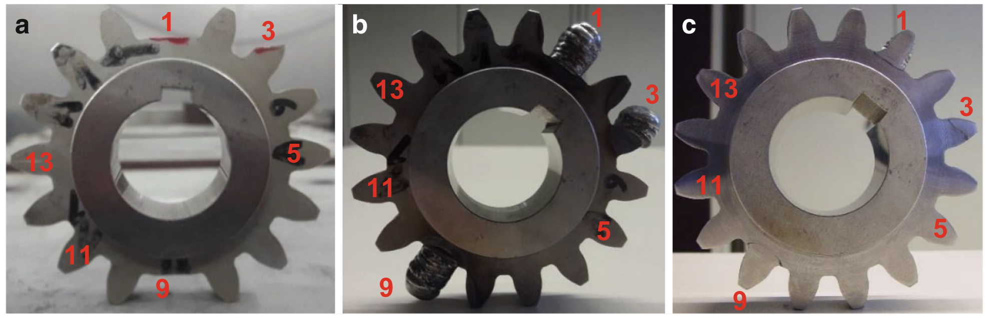

Fig. 6 FZG-C, type C-GF Gear Sample. **a** Teeth removed, **b** DLD deposition and **c** Reshape teeth profile

can cause the gear quality grade to decrease. As an illustration, the gear quality grade would be equal to 6 (R_s= 0.012 mm) if only the teeth away from the DLD (3, 7, 11, and 15) are considered. In addition, the average roughness of teeth flanks obtained with this approach was equal to 0.9 µm and the maximum pitch deviation from the reference value (p_n = 14.137 mm) was 0.117 mm.

Finally, in addition to the EMD post-processing, the gear faces have been turned to remove excess material in the front and back due to the deposited prism dimensions.

2.2 FZG gear tests

The FZG gear test equipment is illustrated in Fig. 9 and well described in ISO 14635-1 [21]. Nonetheless, the test rig uses a power loop principle to impose a constant torque over the tested gears. The shaft attached to the test pinion (1) includes a load clutch (4) where weights on a loading lever (6) produce a fixed torque on the system [22].

The load stages used in the test campaign, using an arm lever of 0.35 m, as well as the Hertzian contact pressure at the pitch point, are presented in Table 4. The FZG gear tests used a constant rotation speed applied to the wheel of 420 rpm, which means a 630 rpm rotational speed in the pinion and a circumferential velocity at the working pitch circle of 2.4 m/s. Each load stage was tested for 8 h, equivalent to 302,400 cycles on the pinion. The cumulative cycles are also presented in Table 4. The tests utilized a poly-α-olefin (PAO) ISOVG 150 gear oil at 80 ◦C under dip lubrication in the whole set of tests. The lubricant's physical properties are listed in Table 5. Once this test campaign was finished, one decided to proceed with a final endurance evaluation.

Table 3 Direct Laser Deposition process parameters

DLD Parameter	Reference value
Scanning speed	6.0 mm/s
Laser power	1800 W
Powder feed rate	12.0 g/min
Layer height	1.7 mm
Deposition track width	1.8 mm
Deposition track overlap	0.30
Perimeter-core idle time	10 s
Inter-layer idle time	27 s
Carrier gas	4.0 l/min—AISI 413
	2.5 l/min—Inconel 625
Shielding gas	26.0 l/min

Table 2 Materials chemical composition (nominal wt. %)

	Ni	Cr	Mo	Nb	Fe	Other
Inconel 625	58–63	20–23	8–10	3–5	≤5	<2
	Fe	**Cr**	**Ni**	**C**		
AISI 431	Balance	17	2	0.18		

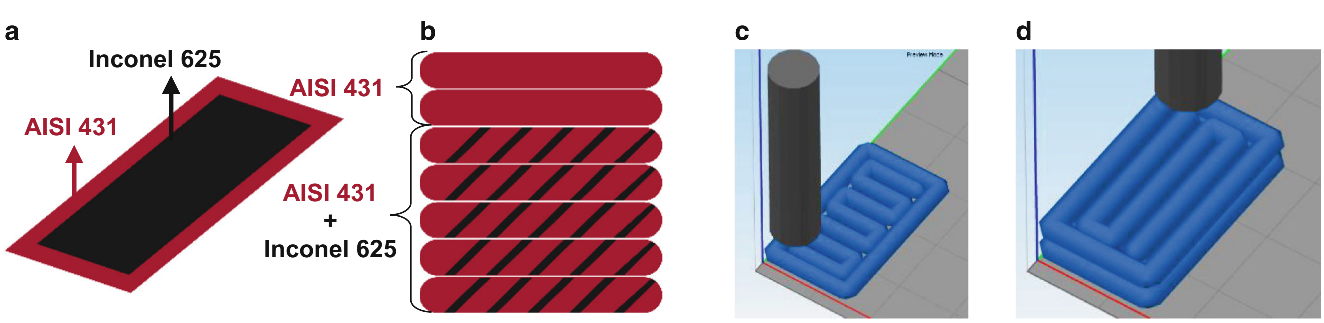

Fig. 7 DLD strategy for gear tooth reconstruction. **a** materials distribution in a single layer, **b** material layer stacking sequence, **c** laser scanning pattern I and **d** laser scanning pattern II

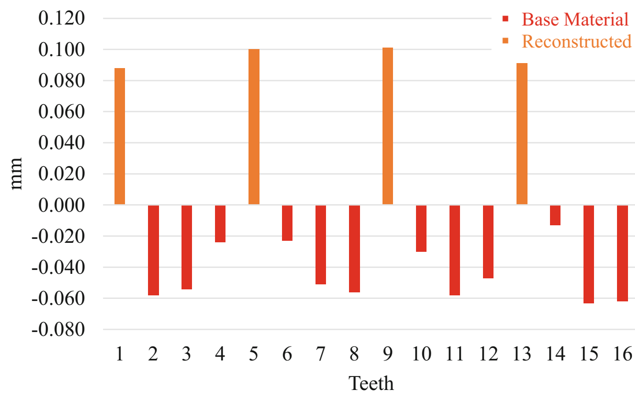

Fig. 8 Tooth thickness errors for a FZG-C Type C-GF pinion reconstructed with DLD

Table 4 Load stages used in the FZG test campaign

Load stage	Pinion torque	Hertzian pressure at pitch point	Cumulative cycles on pinion
K1	3.3 Nm	0.17 GPa	302,400
K2	13.7 Nm	0.35 GPa	604,800
K3	28.8 Nm	0.51 GPa	907,200
K4	46.6 Nm	0.65 GPa	1,209,600
K5	70.0 Nm	0.80 GPa	1,512,000
K6	98.9 Nm	0.95 GPa	1,814,400
K7	132.5 Nm	1.10 GPa	2,116,800
K8	171.6 Nm	1.25 GPa	2,419,200
K9	215.6 Nm	1.40 GPa	2,721,600

Table 5 PAO ISO VG 150 gear oil properties Adapted from [22]

Base Oil Parameter	Reference value
Kinematic viscosity @ 40 °C	152.0 cSt
Kinematic viscosity @ 70 °C	46.5 cSt
Kinematic viscosity @ 100 °C	18.9 cSt
Density @ 15 °C	0.854 g/cm^3

In this sense, a K14 load stage test was performed using an arm lever of 0.50 m, which means a 716.0 Nm torque on the pinion and a 2.549 GPa Hertzian contact pressure at the pitch point. This particular choice relies on the idea that the base material (16 MnCr 5) under such circumstances presents at the end of eight hours (302,400 cycles) a safety factor of 0.991 against tooth root fatigue fracture. In this way, it would be possible to evaluate the behaviour of the reconstructed teeth in a limiting condition of the base material, which is well-known and specified, different from the DLD materials, which still have limited information available.

It is worth mentioning that this is not a standardised test. Since this is exploratory work and for the first time a reconstructed gear would be actually tested, a very conservative load stage sequence was chosen to evaluate the reconstructed teeth. The idea was to employ a campaign where root strength and flank degradation could be gradually assessed.

2.3 Test evaluation

At the end of each load stage, the pinion was cleaned using an ultra-sound bath with petroleum ether for 15 min. Then, mass and tooth flank roughness were measured, as well as visual inspection registered via pictures.

A scale with 0.001 g resolution was used for the pinion mass assessment. A reference mass (mr) of (502.529 ± 0.001) g was also weighed in every evaluation in order to dismiss scale calibration issues in the pinion mass measurements. The mass loss (Δm) was calculated using Eq. 1, where any deviation in the reference mass is also attributed to the pinion under the test [22]. However, since the reference mass variations were consistent with the scale resolution, it is safe to assume that the pinion mass did not

Fig. 9 FZG test rig. Adapted from [22]

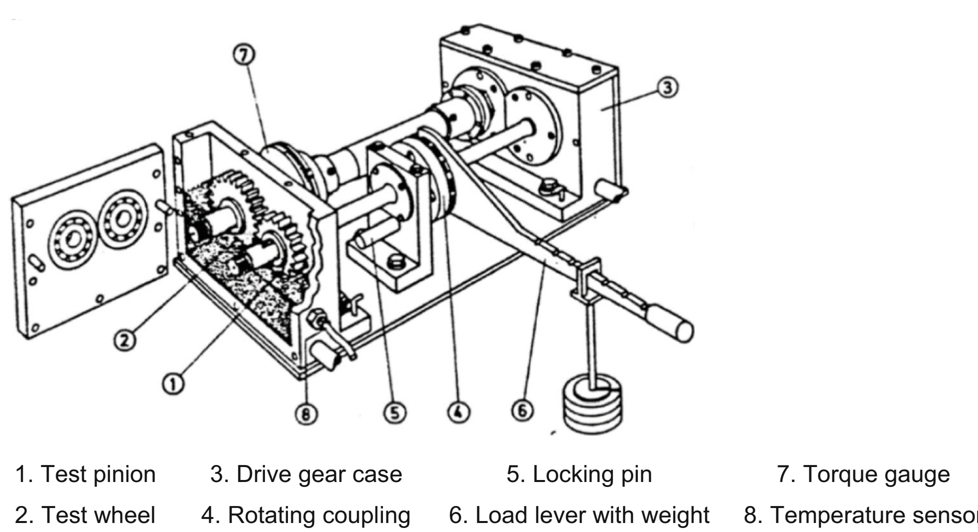

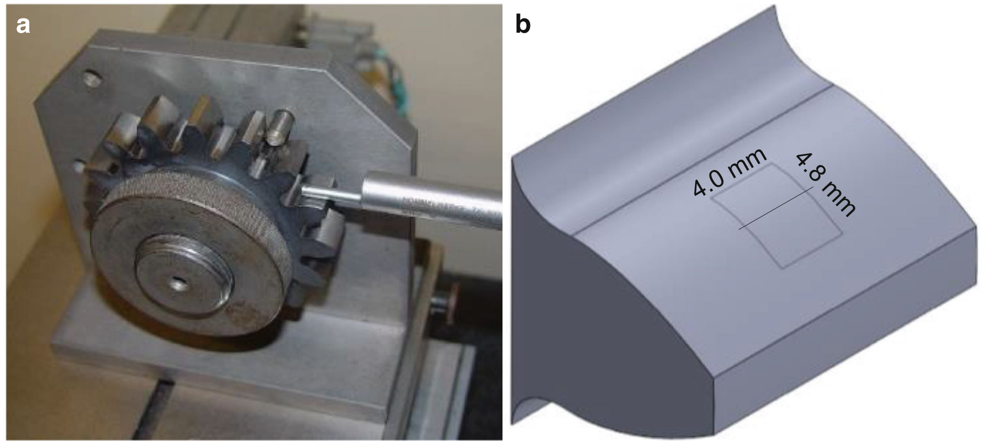

Fig. 10 Surface roughness measurement. **a** Pinion position and **b** rectangular area location

change due to any scale calibration problems but only due to the performed tests.

$$\Delta m(m_{i+1} - m_i) + (mr_{i+1} - mr_i) \quad (1)$$

A Hommelwerke T8000 controller was used to measure the teeth's flank surface roughness following recommendations in ISO 21920-2 [23]. A TK300 pickup with a cone angle of 90°, a tip radius of 5 µm, and a vertical measuring range of ±300 µm was employed in a 4.8 mm × 4.0 mm rectangular area (measured in the profile direction with 400 acquisitions and lateral resolution of 0.01 mm), as indicated in Fig. 10b. A fifth-degree polynomial was used to remove the tooth form and a Gaussian regression filter with a cut-off length of 0.8 mm was selected based on the teeth flank roughness value. Once more, teeth 1, 3 and 9 represent the reconstructed teeth behaviour throughout load stages, while teeth 5, 11 and 13 are the base material reference.

Finally, a Digital Camera was used to take photos and record the visual inspection, keeping the pictures' light intensity and teeth position constant.

3 DLD teeth considerations

Before getting into the results from the FZG test campaign, four aspects of the reconstructed teeth came to the fore and should be discussed.

1. The turning post-processing to restore the teeth' face width produced a series of defects over the DLD teeth' edges, as illustrated in Fig. 11 by the black arrows. The intermittent shocks between the cutting tool and the gear led to inappropriate material removal.
2. A Liquid Penetrant Inspection revealed several crack defects on the DLD teeth prior to any test, probably related to the deposition process itself, as shown in Fig. 12a (pink marks in reconstructed tooth 1). On the other hand, the base material did not present a similar problem as demonstrated in Fig. 12b.
3. The dimensions of the DLD prism proved inappropriate for the EDM strategy employed in the geometric teeth restoration. As schematically represented in Fig. 13, part of the core was exposed after the wire cut, producing a material transition zone Inconel 625/AISI 413 over the teeth flanks.
4. A preliminary hardness assessment performed on the top of each tooth (over the tip diameter) disclosed a reduction in the reference value (766 HV1) for the teeth close to the DLD process, as one can see in Fig. 13. Still, teeth further away from the DLD process were not thermally affected and kept the original hardness. Finally, the deposited AISI 413 presented about 30% lower hardness than base material teeth, while the exposed Inconcel 625 had a value of 295 HV1.

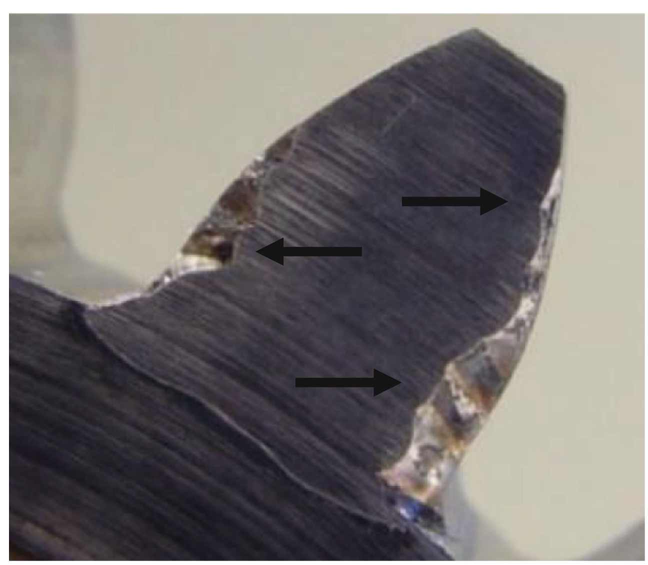

Fig. 11 Tooth 1 defect due to turning post-processing

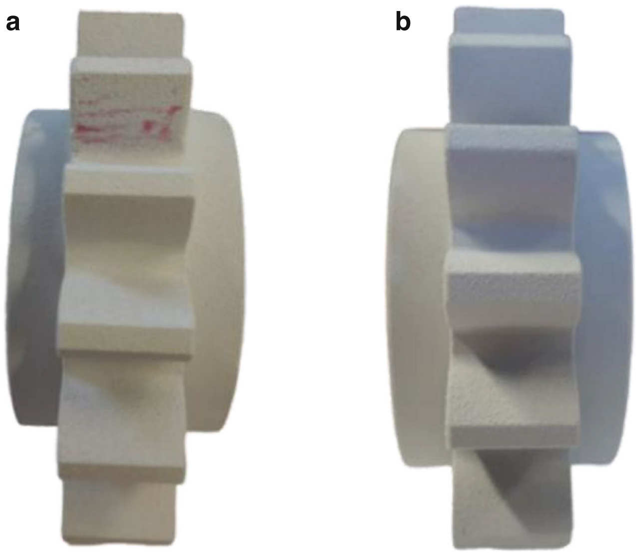

Fig. 12 Liquid Penetrant Inspection for crack defects. **a** Reconstructed tooth 9 with cracks and **b** Material base teeth free of defects

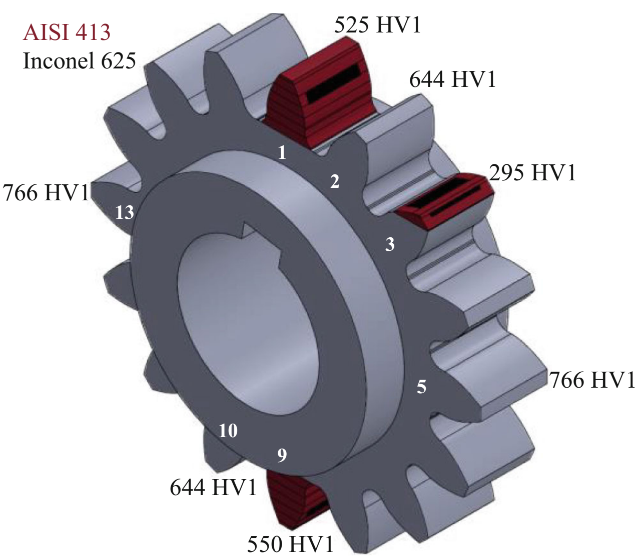

Fig. 13 Material transition zone over the tooth flanks: AISI 431 in red and Inconel 625 in black. Hardness assessment after DLD

5. In order to confirm the material transition zone (item 3) and the results from the preliminary hardness evaluation (item 4), once the FZG test campaign was completed, the reconstructed tooth 9 was removed from the gear and cross-sectioned to allow an internal assessment of the DLD. The microhardness values, indicated in Fig. 14, were measured in a central line and along the involute profile of the active flank. The central line measurements showed three levels of hardness: a higher one at the top of the tooth, equal to 453 HV0.2, referring to AISI 413; a second region referring to Inconel 625, whose average is 242 HV0.2; and the third area associated with the base material (16 MnCr 5), with an average value of 308 HV0.2. There is a slight difference between the hardness of Inconel 625 at the top of the tooth and the root of the tooth, with an increase in values for the depositions close to the base material. For the measurements along the involute profile, it is worth highlighting the evident change in hardness in the transition from AISI 413 to Inconel 625 (369 HV0.2—218 HV0.2) and back to AISI 413 (279 HV0.2—310 HV0.2), which corroborates with Inconel 625 core exposing hypotheses (item 3).

Fig. 14 Tooth 9 cross-section microhardness (HV0.2)

4 FZG test results and analyses

4.1 Teeth flank durability

4.1.1 Mass loss results

Figure 15 presents the mass loss throughout the FZG load stages used to evaluate the pinion performance. Between stages K1 and K5, no significant mass loss was detected. As one can see, the most significant mass change occurred in K8 (89 mg), and a total of 170 mg were removed from the pinion at the end of nine load stages. At this point, this first exploratory work did not replicate the same operating condition in a non-restored pinion in order to promote straightforward comparison. However, safeguarding the due differences in the FZG test conditions presented by [22], it can be said that the reconstructed pinion showed a more significant mass loss than pinions in only base material.

For instance, Fernandes et al. [22] performed a K9 load stage for 8 h at 80 ◦C, using a similar base material pinion, and obtained a mass loss of only 14 mg.

4.1.2 Roughness results

Figure 16 shows the evolution of seven areal roughness parameters throughout the FZG tests, namely: Arithmetical Mean Height (S_a), Root Mean Square Height (S_q), Maximum Peak Height (S_p), Maximum Pit Height (S_v), Maximum Height (S_z), Skewness (S_{sk}) and Kurtosis (S_{ku}) [24].

In these charts, one can see the average and standard deviation obtained for the reconstructed (R) teeth 1, 3 and 9, as well as the average and standard deviation for the base material (BM) teeth 5, 11 and 13.

From the tooth flank roughness parameter perspective, which can be used to assess the surface condition, there is a clear difference between R and BM teeth development in the different load stages. While BM kept roughness parameters constant and stable, slightly decreasing along the tests, R presented significant changes, starting at the K5 load stage, leading to an increase in all roughness height parameters. Particularly S_p, S_v and S_z proved to be sensitive tooth flank surface evolution and damage, with a more pronounced detachment of the curves BM and R.

Since S_p represents the highest peak in the measured area, S_v accounts for the absolute value of the lowest pit and S_z is defined as the sum of the previous two, it is possible to assume that changes in these parameters are directly related to failure occurrence on the flank teeth, and their increase is linked to the failure development. Also, one can mention that S_a and S_q also indicated changes in the teeth' surface condition, but these modifications manifested only in subsequent loading stages.

Finally, Skewness (S_{sk}) and Kurtosis (S_{ku}) are parameters related to roughness shape and distribution. Skewness is a measurement of the profile's symmetry around the mean line. This parameter can be affected by deep valleys or high peaks. A height distribution with as many peaks as valleys has zero skewness, while profiles with deep scratches or removed peaks have negative skewness. The kurtosis describes the sharpness of the probability density of the profile. $S_{ku} > 3$ indicates that the distribution curve has relatively many high peaks and low valleys [25].

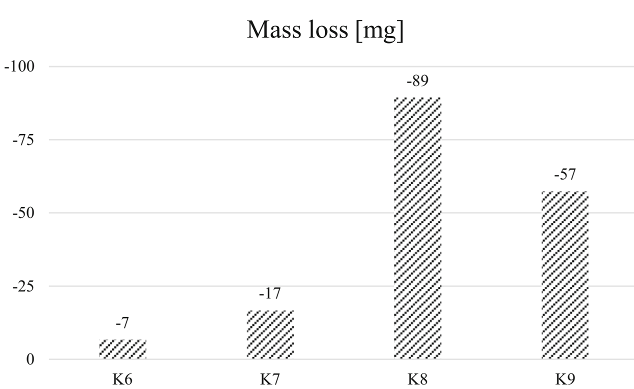

Fig. 15 Mass loss throughout load stages

4.1.3 Visual inspection results

Figure 17 presents a collection of images for teeth 1, 3 and 9, where the evolution of the flank condition can be observed throughout the nine load stages. Similarly, Fig. 18 shows the development of the flanks of teeth 5, 11 and 13 for the base material.

The first point to observe is the already mentioned Inconel 625 core exposing after the wire cut, producing a material transition zone Inconel 625/AISI 413 over the teeth flanks, as indicated by the continuous black arrow in Fig. 17. Also, Fig. 17 puts in evidence the high level of degradation suffered by the reconstructed teeth throughout the nine loading stages, namely spalling (dashed grey arrow) and scuffing (continuous grey arrow). In addition, one can see in tooth 9 a severe plastic deformation (continuous white arrow), where its limits "broaden". A reasonable hypothesis for the mentioned problems resides in the fact that both DLD materials have lower hardness values than the base material teeth on the wheel. Although the reconstructed teeth allowed the gear to perform the proposed FZG gear tests, there is no doubt that they presented significant failure developments.

On the other hand, the images confirm that the base material case-hardened 16 MnCr 5 withstood the test campaign, presenting at the end of the K9 stage, mostly micropitting in the root of the teeth (dashed white arrow). It should also be mentioned that since this pinion has a history of tests, it already showed signs of micropitting in K1, with regular development through the tests.

4.2 Endurance test

As previously indicated, the endurance test using a K14 load stage sought to compare the reconstructed teeth against the base material limit (302,400 cycles), assessing the tooth root resistance. However, at the end of only 36,900 cycles, the pinion presented catastrophic failure, interrupting the test. Figures 19 and 20 present the results for the endurance test.

As shown in Fig. 19, DLD tooth 1 and base material tooth 2 fractured at the root. Considering the active flank, it can be assumed that the reconstructed tooth 1 was the first to fail, causing an overload on the base material tooth 2, leading to its rupture. Tooth 3, partially reconstructed, also showed severe damage and, in particular, loss of adhesion to the base material, as indicated by the black arrow in

Fig. 16 Roughness parameters throughout load stages. *BM* Base material, *R* Reconstructed

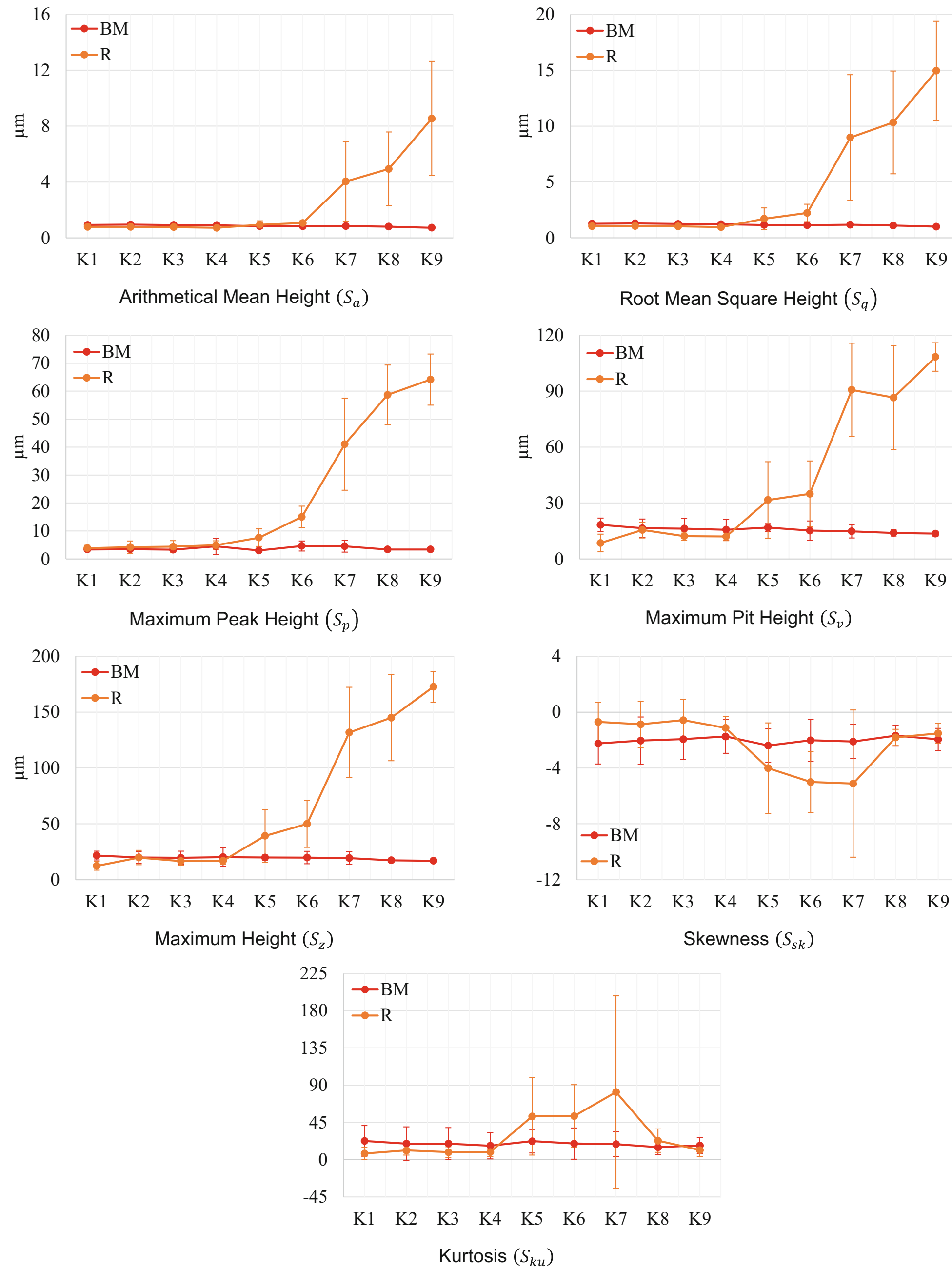

Fig. 19b. Tooth 9 showed significant wear, namely scuffing at the tooth tip.

A highlight in this analysis is the degradation presented by teeth 10 and 11 after the K14 load stage. As illustrated in Fig. 20, the base material tooth 10 showed both spalling on its flank (dashed grey arrow) and scuffing (continuous grey arrow), similar to what was observed in tooth 9. Base material tooth 11 presented scuffing on its face, indicated by the grey arrow. It can be assumed that the hardness reduction due to the thermal effects of the DLD led to the weakening of these teeth, producing the results. This argument is corroborated by the better aspect presented by teeth 5 and 13 since these teeth were further away from the DLD.

5 Main findings

Based on what was presented, some findings from this research should be highlighted:

- First, it was possible to truly reconstruct a damaged gear using DLD. In this sense, the restoration procedure included the cleaning step (teeth machining removal), the

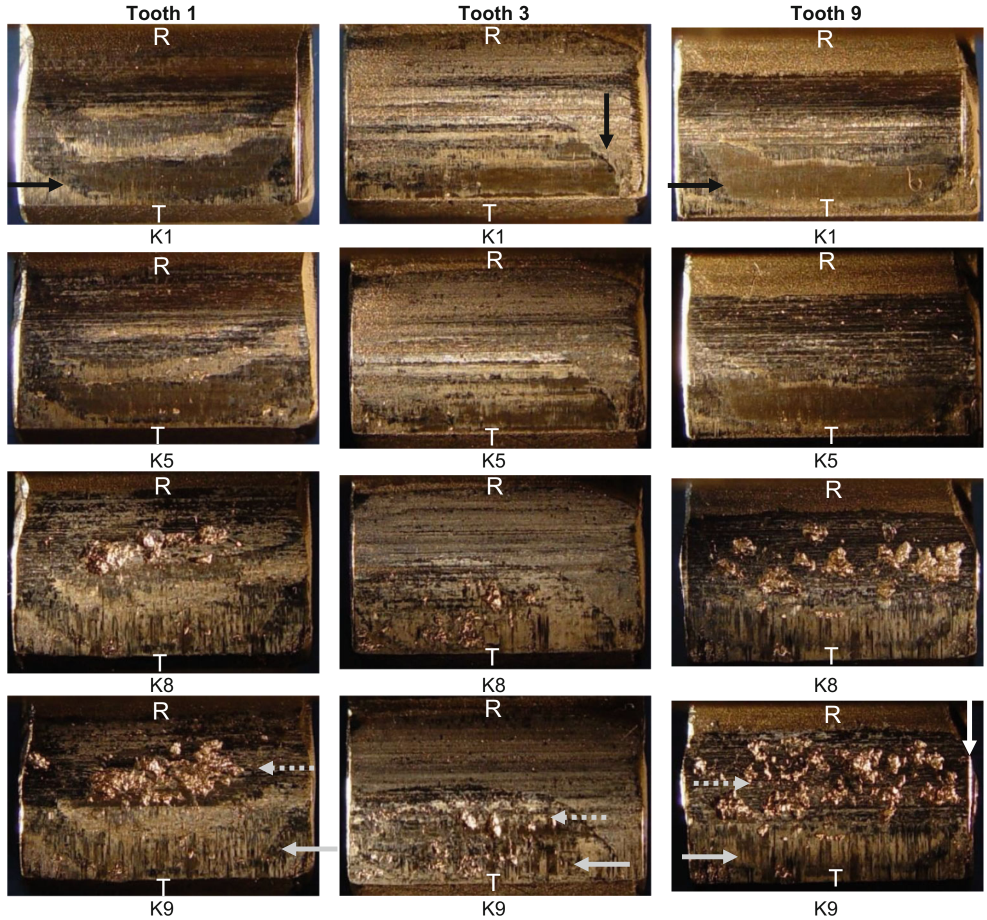

Fig. 17 Reconstructed teeth evolution throughout load stages, *R* tooth root, *T* tooth tip

deposition step (using a combination of two materials) and the finishing step (the tooth's involute profile was achieved by employing wire EDM and the gear teeth width restored by turning).

- Second, it was possible to carry out a series of functional tests. That is, the reconstructed pinion actually worked up to a 215.6 Nm load stage torque (there are no similar results in the technical literature until now). Undoubtedly, the FZG test campaign was significantly more aggressive for the DLD teeth than for the base material. The degradation suffered in teeth 1, 3 and 9 was evident in the roughness parameters, where quite distinct trends and evolutions could be observed in the base material and the DLD teeth, as well as in the visual record that compares them. It is plausible to assume that the exposure of Inconel 625 after EDM cutting and the lower hardness of the deposited materials compared to the base material are related to the problem. Concerning the failure mechanisms involved, visual inspection revealed spalling and scuffing in the reconstructed teeth. It is also important to highlight that tooth 9 presented plastic deformation starting at load stage K8, where its limits, in fact, "broaden". On the other hand, the base material teeth showed only micropitting in the root of the teeth, with regular area evolution throughout stages K1 to K9.
- Finally, concerning resistance to breakage at the base of the tooth, it can be said that up to stage K9, very good results were observed, with the reconstructed teeth showing satisfactory adhesion to the base material and resistance. However, the endurance test at K14 proved catastrophic to the gear, with the complete tooth root breakage of teeth 1 and 2 after 36,900 cycles. This test also revealed that the base material teeth near the DLD performed worse than those far from the deposition. It can be assumed that the thermal effects in the teeth close to the DLD cause the problem.

6 Conclusion

This exploratory work detailed the strategy used to restore a base material case-hardened 16 MnCr 5 an FZG-C Type C-GF pinion using a DLD combination of pure Inconel 625 (MetcoClad 625) for the tooth core and pure AISI 431 (Metco 42C) as a superficial coating, showed that it is possible to test a reconstructed gear under actual operational conditions and compared its performance against

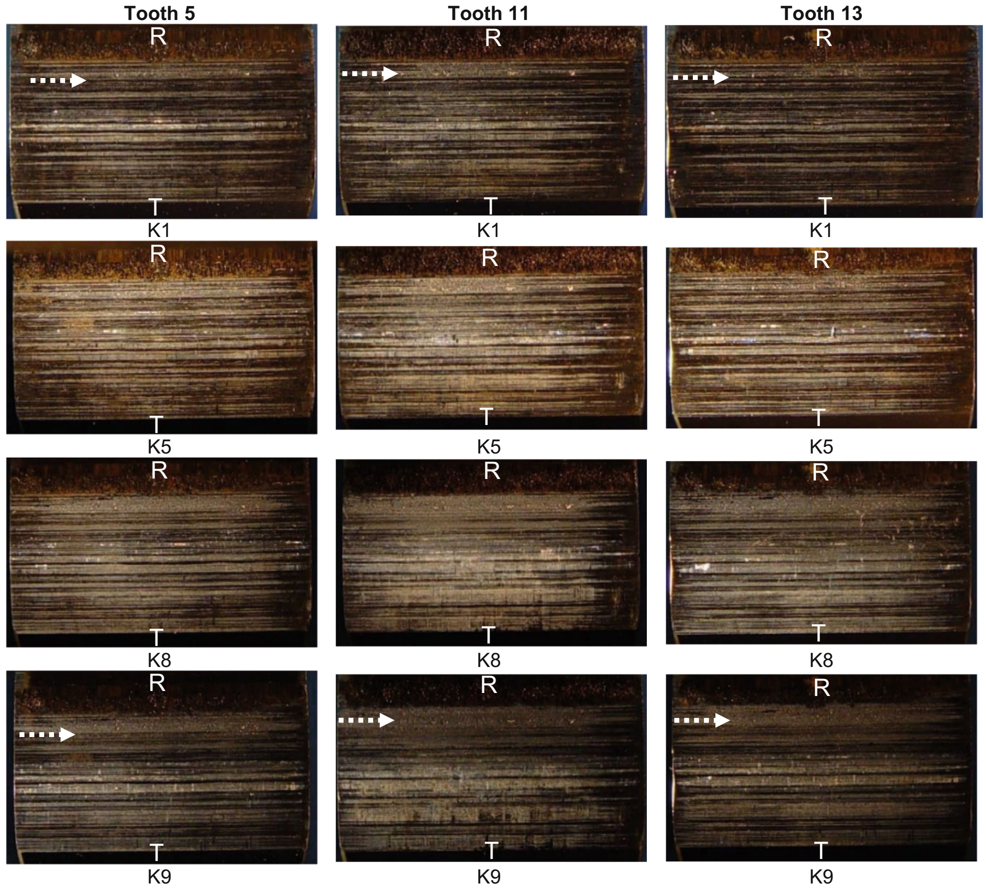

Fig. 18 Base material teeth evolution throughout load stages, *R* tooth root, *T* tooth tip

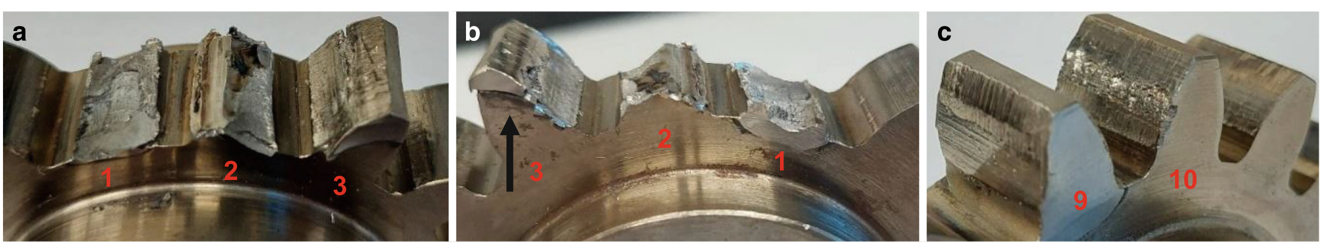

Fig. 19 DLD reconstructed gear after the K14 load stage. **a** front view for teeth 1, 2 and 3; **b** back view for teeth 1, 2 and 3; **c** front view for teeth 9 and 10

the base material. In this sense, the choice of two materials, one for the core with good build-up capabilities and the other for the coating with higher hardness, proved feasible and effective in producing a tooth with an involute profile capable of being tested.

About the two aspects investigated in the reconstructed teeth, tooth root resistance and flank durability, it should be noted that both were inferior to those presented by the base material. This is also why the term reconstructed and not repaired was chosen when referring to teeth obtained via DLD in this work. Even so, concerning the adhesion of the rebuilt tooth to the base material, there is much merit in the results obtained, given that the K9 stage already introduces loads at the base of the tooth similar to several actual operations. On the other hand, the durability of the flank proved to be far below what is necessary for a practical gear application. In this sense, two main failure mechanisms were identified, spalling and scuffing, which can be attributed to the hardness of the AISI 413 material being lower than the hardness of the base material 16 MnCr 5, the transition zone between Ionconel 625/AISI 413 after cutting by EDM and the change in the tooth profile itself as a result of the wear observed throughout the tests.

This exploratory work taught that caution is needed when planning the deposition prisms' dimensions to not compromise the teeth' flank capabilities. For this specific case, a miss calculation led to the mentioned Inconel 625/AISI 413 transition problem, and so a human error might be

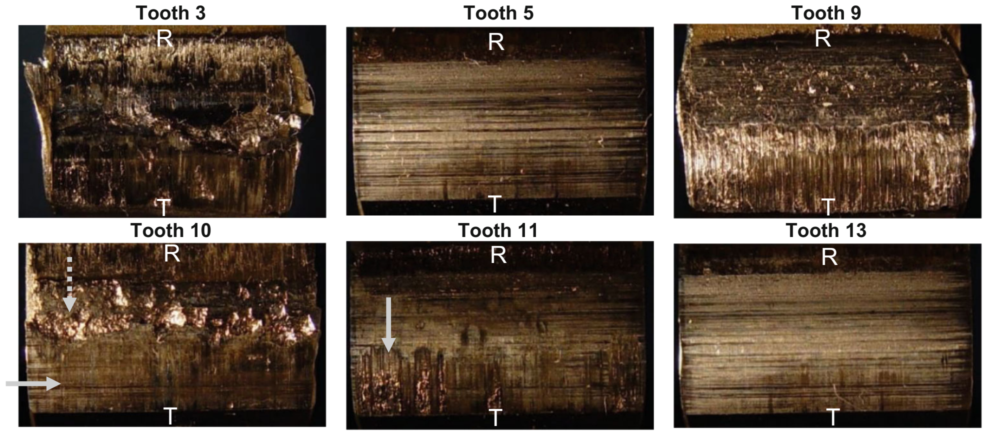

Fig. 20 Teeth aspect after load stage K14, *R* tooth root, *T* tooth tip

seen as the primary cause here. Therefore, it is important to record some recommendations for future studies related to the reconstruction of gear teeth via DLD:

- Selection of a material for the coating of the tooth with better contact fatigue and wear capacity than AISI 413, that is, higher hardness levels. In this context, it is necessary to identify process parameters that guarantee the integrity of the coating and minimize cracks arising from the DLD, such as those observed with penetrating liquid;
- Perform a detailed analysis of the deposition geometry to not repeat the mistake in this first study, where Inconel 625 was exposed;
- Use other forms of machining in the post-processing of the deposited tooth, mitigating intermittent shocks with the cutting tool that could damage the reconstructed teeth (e.g., using milling instead of turning);
- Thermally protect the base material teeth close to the DLD zone to not weaken these adjacent teeth.

Finally, about the state of the art, this work contributed to presenting results of real tests in gears reconstructed via DLD, something that until now had not been seen, with a strategy that produced a tooth capable of being tested in an FZG test rig. These results can now be used as a reference for new reconstructions and a basis for comparison.

Acknowledgements The authors gratefully acknowledge the financial support of several projects and grants, namely:

National Funds through Fundação para a Ciência e a Tecnologia (FCT) under the PhD grant 2021.05562.BD;

GEAR3D under project POCI-01-0247-FEDER-039848;

LAETA under project UID/50022/2020

Conflict of interest P.C. Romio, P.M.T. Marques, J.H.O. Seabra, C.M.C.G. Fernandes, J. Gil, R. Cardoso, M.F. Vieira and J.M. Cruz declare that they have no competing interests.

References

1. International Standard ISO 10825 – 1: Gears—Wear and damage to gear teeth—Part 1: Nomenclature and characteristics, Reference number ISO 10825-1:2022 (E), Published in Switzerland. 2022
2. Michaud M, Sroka GJ, Benson RE (2010) A novel approach to the refurbishment of wind turbine gears. Technical paper 10FTM03. American Gear Manufacturers Association, Virginia
3. Albertini H, Gorla C, Rosa F (2016) A new approach to repair large industrial gears damaged by surface degradation—the refurbishment using the modification of both the profile shift coefficient and the pressure angle. Technical Paper 16FTM23. American Gear Manufacturers Association, Virginia
4. Nikam SH, Jain NK (2017) Laser-based repair of damaged dies, molds, and gears. In: Gupta K (ed) Advanced manufacturing technologies. Materials forming, machining, and tribology. Springer, Cham https://doi.org/10.1007/978-3-319-56099-1_6
5. Liu Q, Djugum R, Sun S, Walker K, Choi Y, Brandt M (2017) Repair and manufacturing of military aircraft components by additive manufacturing technology. In: Proceedings of the 17th Australian International Aerospace Congress (AIAC 2017) Melbourne
6. Mahamood RM (2017) Areas of application of laser metal deposition process—part repair and remanufacturing. Laser metal deposition process of metals, alloys, and composite materials. Springer, Cham https://doi.org/10.1007/978-3-319-64985-6_7
7. Saboori A, Aversa A, Marchese G, Biamino S, Lombardi M, Fino P (2019) Application of directed energy deposition-based additive manufacturing in repair. Appl Sci 9(16):3316. https://doi.org/10.3390/app9163316
8. Thompson SM, Bian L, Shamsaei N, Yadollahi A (2015) An overview of direct laser deposition for additive manufacturing; part I: transport phenomena, modelling and diagnostics. Addit Manuf 8(27):36–62. https://doi.org/10.1016/j.addma.2015.07.001
9. Shi J, Bai SQ (2013) Research on gear repairing technology by laser cladding. Key Eng Mater 546(5):40–44. https://doi.org/10.4028/www.scientific.net/KEM.546
10. Zhu L, Wang S, Pan H, Yuan C, Chen X (2020) Research on remanufacturing strategy for 45 steel gear using H13 steel powder based on laser cladding technology. J Manuf Process 49(11):344–354. https://doi.org/10.1016/j.jmapro.2019.12.009
11. Bons M (2020) Gear repair using laser metal deposition. TU Delft Mechanical, Maritime and Materials Engineering, Delft (Master of Science thesis)
12. Guan C, Yu T, Zhao Y, Chen L, Chen Y (2023) Repair of gear by laser cladding Ni60 alloy powder: process, microstructure and me-

chanical performance. Appl Sci 13(1):319. https://doi.org/10.3390/app13010319
13. Faculty of Engineering of the University of Porto (FEUP) Gear3D-3D reconstruction of large gear teeth via direct laser deposition, POCI-01-0247-FEDER-039848. https://sigarra.up.pt/feup/en/PROJECTOS_GERAL.FICHA_PROJECTO?p_id=74562
14. Ferreira AA, Darabi R, Sousa JP, Cruz JM, Reis AR, Vieira MF (2021) Optimization of direct laser deposition of a Martensitic steel powder (Metco 42C) on 42crMo4 steel. Metals 11(4):672. https://doi.org/10.3390/met11040672
15. Ferreira AA, Amaral RL, Romio PC, Cruz JM, Reis AR, Vieira MF (2021) Deposition of nickel-based Superalloy claddings on low alloy structural steel by direct laser deposition. Metals 11(8):1326. https://doi.org/10.3390/met11081326
16. Ferreira AA, Reis AR, Amaral RL, Cruz JM, Romio PC, Seabra JHO, Vieira MF (2022) Mechanical and microstructural characterisation of bulk Inconel 625 produced by direct laser deposition. Mater Sci Eng A 838:142777. https://doi.org/10.1016/j.msea.2022.142777
17. Ferreira AA, Reis AR, Sousa JP, Romio PC, Cruz J, Seabra JHO, Vieira MF (2021) Functionally graded materials fabricated by direct laser deposition for gear repair. 2nd International Conference on Advanced Joining Processes, Sintra
18. Romio P, Marques PMT, Fernandes CMCG, Seabra JHO (2022) Analysis of the rolling contact fatigue performance of direct laser deposition repairs for wind turbine gearbox applications. Porto-Lyon Seminar 2021, Lyon. https://doi.org/10.24840/978-972-752-293-4
19. Romio P, Marques PMT, Fernandes CMCG, Cruz JMB, Seabra JHO (2022) Assessment of the rolling contact fatigue performance of discs repaired via direct laser deposition. 5th Meeting of the Young Researchers of LAETA, Lisbon
20. Forschungsvereinigung Antriebstechnik EV (1993) Test procedure for the investigation of micropitting capacity of gear lubricants. FVA Information Sheet, Research Projects Nr. 54/I–IV
21. International Organization for Standardization, Gears—FZG test procedures—Part 1: FZG test method A/8,3/90 for relative scuffing load-carrying capacity of oils (ISO 14632-1:2000), 2000.
22. Fernandes CMCG, Pais JC, Martins RC, Seabra JHO (2021) Influence of running-in operating conditions on the steady-state torque loss of ground spur gears. Forsch Ingenieurwes 85(16):567–582. https://doi.org/10.1007/s10010-021-00447-0
23. International Standard ISO 21920-2.: Geometrical product specifications (GPS)—Surface texture: Profile—Part 2: Terms, definitions and surface texture parameters. 2021.
24. Blateyron F (2013) The areal field parameters. In: Leach R (ed) Characterisation of areal surface texture. Springer, Berlin https://doi.org/10.1007/978-3-642-36458-7_2
25. Cuffaro V (2013) Prediction method for the surface damage in splined couplings. Politecnico di Torino, Torino (PhD. Thesis in Mechanic)